

Observational consequences of a dark interaction model

M.de Campos⁽¹⁾

November 8, 2018

1

Abstract

We study a model with decay of dark energy and creation of the dark matter particles. We integrate the field equations and find the transition redshift where the evolution process of the universe change the accelerated expansion, and discuss the luminosity distance, acoustic oscillations and the statefinder parameters.

Keywords: Dark matter, dark energy, luminosity distance, acoustic oscillations, statefinder parameters.

1 Introduction

Before the results from supernova of the type IA observations appear in the literature, that indicates an accelerated expansion of the universe, L. Krauss and M. Turner have called our attention that “The Cosmological Constant is Back”. They cited the age of the universe, the formation of large scale structure and the matter content of the universe as the data that indicates the insertion of cosmological constant [1]. The cosmic microwave background radiation anisotropy and large scale structure, also indicates this acceleration expansion of the universe [2]- [4]. Besides, the analysis of 158 SNe realized by Riess et al. [5] point out the present acceleration ($q < 0$) at 99.2% at confidence level.

The mechanism that triggered the acceleration of the universe has not been identified, and the simplest explanation for this process is the inclusion of a non null cosmological constant. However, the inclusion of cosmological constant creates new problems. Some of them are old, as the discrepancy among the observed value for the energy density

¹Physics Department - Roraima Federal University. Av. Ene Garcez 2413, Campus do Paricarãna, Bloco V, Bairro Aeroporto, Boa Vista, Roraima, Brasil.69304-000,email:campos@if.uff.br.

of the vacuum and the large value suggested by the particle physics models [6], [7]. In spite of the problems caused by the inclusion of Λ , the cosmological scenario with Λ has a good agreement with respect to the estimate age of the universe, the anisotropy of the microwave background radiation and the supernova experiments. Besides, making several assumptions concerning with the spectrum of fluctuations in the early universe and the formation of the galaxies, G. Efstathiou suggests that the small value of cosmological constant can be explained by the anthropic principle [8]. Although the inclusion of Λ is the simplest explanation for the cosmic acceleration, there are a lot of alternatives to explain the accelerated expansion. See the reviews [9] and [10], and the references therein. So, we have experimental evidence for two extra components for the universe. One is responsible for the cosmic acceleration and represents about 70% of material content, and the other acts gravitationally as ordinary matter, but is not baryonic.

The evidence that these new components of the universe, dark matter and dark energy are different substances has been considered in the literature [11]. Generally, the dark matter component is considered as weakly interacting massive particles and the dark energy component is associated to some form of a scalar field. A link between both components to a scalar field is studied by Padmanabhan and Choudhury [12]. Although, today, both components are unknown in respect to the their nature.

An alternative model that furnish a negative pressure in the cosmic fluid and results in an accelerated expansion of the universe is known as open system cosmology (OSC) [13]. In OSC model the particle number in the universe is not conserved and the energy-momentum tensor is reinterpreted in the Einstein's field equations, where appear an extra negative pressure known as creation pressure [14], [15]. The creation process is due to the expenses of the gravitational field and is an irreversible process. One of the attractive features of the hypothesis of particle production in OSC model is the relation among the large scale properties of the universe and the atomic phenomena [16].

The coupling into dark matter and dark energy has been considered within three possibilities in literature. First, considering the dark matter decaying in dark energy; second, the dark energy decaying to dark matter; or interaction in both directions. See [17] and references therein for examples for every one of the alternatives.

On the other hand, the second law of thermodynamic favored the second possibility [18], [19]. Consequently, if each component is not conserved individually, the chemical potential of at least one of the dark components is not null [17], differently that appear in [18], [19] where both chemical potentials are zero.

In this work we consider a different rate for diluting of the material components due to decaying of the dark energy into dark particles, as the same way that the authors considered in [20]. Several aspects of

this approach are investigate in [21]. We study the transition of the accelerated expansion of the universe, the luminosity distance and the acoustic scale of the anisotropies of CMB, obtaining a validity interval for the parameter that governs the interaction between the dark components. We finish this study with the statefinder pair $\{r, s\}$ that indicates the proximity of this model with LCDM model. We hope that in the future the statefinder parameter to be useful tools in testing interacting cosmologies.

2 The cosmological model

We consider the space-time as homogeneous and isotropic, characterized by the FRW metric

$$ds^2 = dt^2 - R(t)^2[dr^2 + r^2 d\theta^2 + r^2 \sin^2\theta d\phi^2], \quad (1)$$

and the energy momentum tensor as the usual perfect fluid, given by

$$T_{\mu\nu} = (\rho_{dm} + \rho_{de} + P)u_\mu u_\nu - P g_{\mu\nu}. \quad (2)$$

$P = P_{de} + P_{dm}$ is the total pressure, ρ_{de} is the dark energy density, ρ_{dm} is the dark matter density, while u_μ is the four velocity. Taking into account that the reference system is just the matter filling it, the field equations assumes the form

$$\frac{\ddot{R}}{R} = -\frac{4}{3}\pi G(\rho_{dm} + \rho_{de} + 3P), \quad (3)$$

$$\frac{\dot{R}^2}{R^2} = \frac{8\pi G}{3}(\rho_{dm} + \rho_{de}), \quad (4)$$

where the spatial flatness is assumed, in accord with the data from WMAP [22].

Writing the conservation law as

$$u_\mu T_{;\nu}^{\mu\nu} = -u_\mu(\rho_{de} g^{\mu\nu})_{;\nu}, \quad (5)$$

its assumes the form

$$\dot{\rho} + 3\frac{\dot{R}}{R}\rho = -\dot{\rho}_{de}, \quad (6)$$

where $\rho = \rho_{dm} + \rho_{de}$.

Although the vacuum component decays, we consider that the state equation remains with the usual state equation expression, $P_{de} = -\rho_{de}$. Some details about Λ decaying model can be view in [23], and the thermodynamic behavior in [24].

Considering the creation process, the dark matter density will dilute in a different rate, namely

$$\rho_{dm} = \rho_{dm0} R^{\epsilon-3}, \quad (7)$$

where the positive constant ϵ furnish the deviation from the process without decaying of the dark energy component, and the subscript 0 indicates the present time.

Rewritten Eq. (6) as

$$\frac{d\rho_{dm}}{dR} + 3\frac{\rho_{dm}}{R} = -\frac{d\rho_{de}}{dR}, \quad (8)$$

the integration results

$$\rho_{de} = \rho_{de0} - \frac{\epsilon}{3-\epsilon}\rho_{dm0}[1 - R^{\epsilon-3}]. \quad (9)$$

With auxiliou of Eq. (4), (7) and (9) we find the field equation

$$\dot{R}^2 - K_I R^2 - K_{II} R^{\epsilon-1} = 0, \quad (10)$$

where $K_I = \frac{8\pi G}{3}(\rho_{de0} - \frac{\epsilon\rho_{dm0}}{3-\epsilon})$ and $K_{II} = \frac{8\pi G}{3-\epsilon}\rho_{dm0}$, and the solution is given by

$$R(t) = \left(\frac{K_{II}}{K_I}\right)^{\frac{1}{3-\epsilon}} \left\{ \sinh \sqrt{K_I} \frac{3-\epsilon}{2} t \right\}^{\frac{2}{3-\epsilon}}. \quad (11)$$

Consequently, the Hubble function and the deceleration parameter, as functions of the red-shift, are respectively:

$$H(z) = H_0 \left\{ \frac{3\Omega_{dm0}}{3-\epsilon} [(1+z)^{3-\epsilon} - 1] + 1 \right\}^{\frac{1}{2}}, \quad (12)$$

$$q(z) = -1 + \frac{3-\epsilon}{2} \left\{ \left(1 + \frac{3\Omega_{de}-\epsilon}{3\Omega_{dm}}\right) (1+z)^{\epsilon-3} \right\}^{-1}. \quad (13)$$

The profiles for the Hubble function and deceleration parameter appear in the Fig.1 and Fig.2, respectively.

The age of the universe is one of the observational arguments for the existence of dark components [25]- [27], in spite off, different models with dark energy can furnish the same age for an expanding universe. However, considering the age of the universe at different eras and comparing with the age estimates of high-red shift objects, this degeneracy can be eliminated [29].

The standard FRW model indicates a younger universe, if compared with estimates from globular cluster data [30], and CMB measurements [4]. Using the expression for the Hubble function, given by the Eq.(12), and the correspondent function for the standard model, given by $H_0 = \frac{2}{3t_0}$, we can construct a quotient between these functions, and observe the values for the ϵ parameter that furnish an older universe than the established by the standard model. We find that any positive value for the ϵ -parameter results an older universe. For increasing ϵ we obtain an older universe.

Let's suppose that the universe has the critical density. Using the current value for the Hubble function found by WMAP [22], $H_0 = 73.4_{-3.8}^{+2.8}$

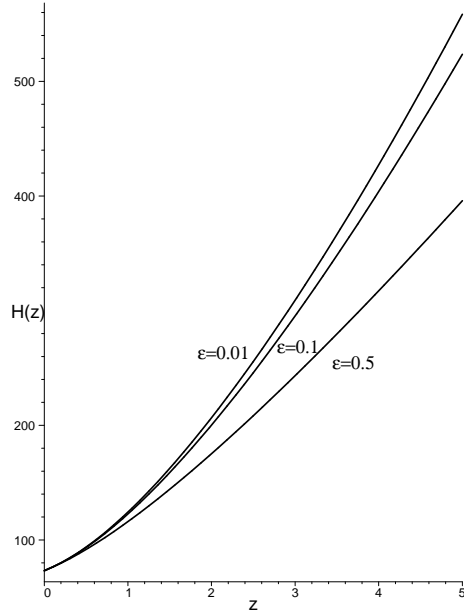


Figure 1: Profile for $H(z) \times z$. The values for ϵ considered are $\epsilon = 0.01, 0.1, 0.5$. Note that the growing value for the ϵ -parameter favored an older universe.

km/s/Mpc, we can estimate a range for t_0 taking into account the FRW standard model, explicitly $t_0 = (8.6 - 9.4)$ Gyr. On the other hand, the experimental data that predicts the age of the globular cluster indicates an interval (10.6-12.27) Gyr [30]. Consequently we have a problem with respect to the age of the universe. Note that, the predict age for the universe around $\epsilon = 0$ is 12.8 Gyr, minimal value for t_0 in this model. So, this model is not plagued with the age problem, since that the age of the globular cluster does not furnish an upper limit to t_0 .

An additional constraint can be obtained using the accelerated process of the universe expansion, that indicates a past deceleration ($q < 0$) beyond the red-shift $z_t = 0.46 \pm 0.13$ at 99.8% at confidence level, where the subscript t refers to the transition point which the universe change the signal of the deceleration parameter. Using the expression for the deceleration parameter (Eq. 13), we can write an expression for the transition redshift, namely

$$z_t = \left\{ \frac{1 - \epsilon}{2} \frac{3\Omega_{dm0}}{3\Omega_{de0} - \epsilon} \right\}^{\frac{1}{\epsilon-3}} - 1, \quad (14)$$

where the profile appear in the (Fig.3). For $\epsilon = 0.01$, we obtain the transition redshift around $z_t = 0.68$, considering $\Omega_{dm} = 0.3$, and $\Omega_{de} = 0.7$.

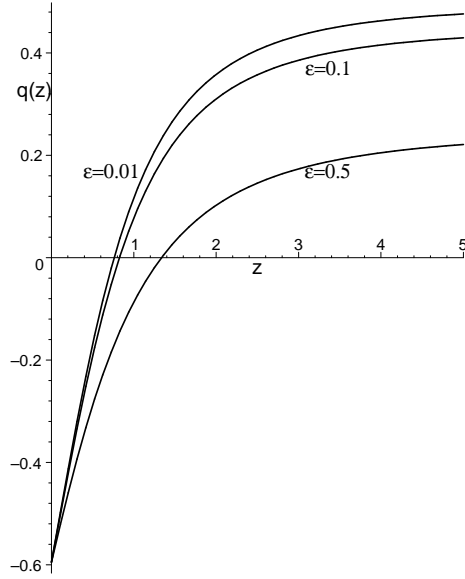


Figure 2: Profile for deceleration parameter as a function of the redshift. Note that the growing value for ϵ results a highest redshift transition. Around the present time, we note by the graph, that the value for the deceleration parameter is $q_0 = -0.59$, inside the interval established in [28] for the present deceleration parameter, namely $q_0 = -0.74 \pm 0.18$.

The expressions (13) and (14) are growing functions of the ϵ -parameter.

3 Luminosity distance and acoustic scale

Considerations about the accelerating expansion of the cosmos and the consequent existence of a dark component comes from geometrical tests that measures the Hubble expansion at various redshifts. One of them is the luminosity distance from standard candles.

The comoving distance $r(t, t_0)$ traveled by a light signal from a time t to the present time is given by

$$r(t, t_0) = \int_t^{t_0} \frac{dt'}{R(t')}, \quad (15)$$

considering flat spatial sections. For redshift as an integration variable we have

$$r(z) = \int_0^z \frac{dz'}{H(z')}. \quad (16)$$

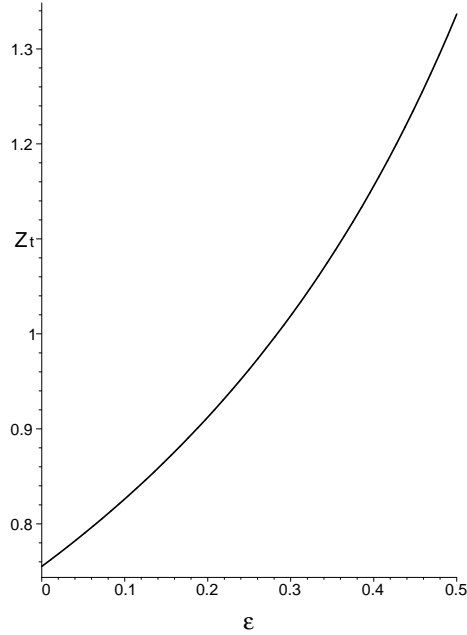


Figure 3: Transition redshift as a function of the ϵ parameter. With increasing of ϵ we obtain an early estimate for the transition redshift, and consequently, an older universe.

With auxilious of the Eqs.(12), we can integrate (16), resulting

$$r(z) = -\frac{H_0}{\Omega_{de0}^2} F_1\left\{\left[\frac{1}{2}, \frac{1}{7-\epsilon}\right], \left[\frac{8-\epsilon}{7-\epsilon}\right], (1+z)^{7-\epsilon} \frac{3\Omega_{dm0}}{(3-\epsilon)\Omega_{de0}}\right\}, \quad (17)$$

where ${}_2F_1$ denotes a hypergeometric function. To illustrate the evolution of the comoving distance for different values for the ϵ -parameter, we show the profile in the (Fig.4).

Indeed, the modulus distance is given by the formula

$$\mu(z) = 5\log\left(\frac{d_L}{Mpc}\right) + 25, \quad (18)$$

where the luminosity distance can be written as

$$d_L = (1+z) \int_0^z \frac{du}{H(u)}. \quad (19)$$

In the Fig.5 we show the profile for the modulus distance versus redshift taking into account $\epsilon = 0.5$, and compare with the Union Sample of 557 Supernova Ia [31] to illustrate the good agreement of the model with respect to the observational data. The profile for different values

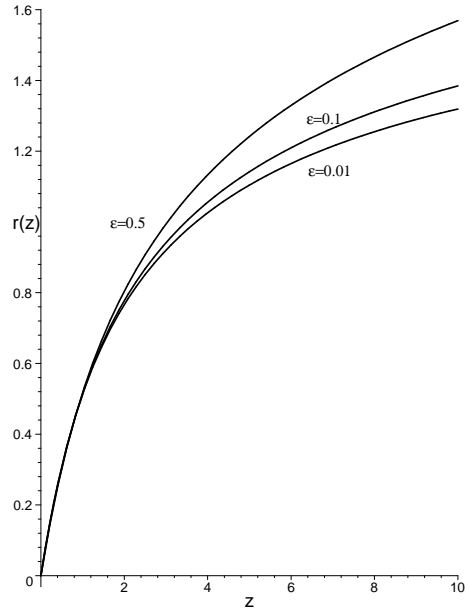


Figure 4: Profile for the luminosity distance versus redshift taking into account $\epsilon = 0.01, 0.1, 0.5$.

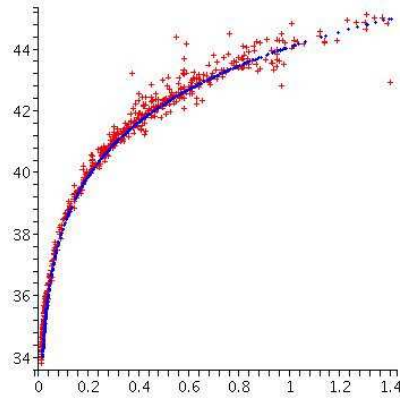


Figure 5: Profile for the modulus distance versus redshift taking into account $\epsilon = 0.5$. The data of the Union Sample of 557 Supernova Ia are the red points and the theoretical results appear as blue points. We consider $\Omega_{de0} \approx 0.7$, $\Omega_{dm0} \approx 0.3$ and the present value for the Hubble constant as 72 km/s/Mpc .

of the ϵ -parameter do not help to decide about the best agreement with SNIa data. Let us see this, performing a chi-square analysis using

$$\chi^2(\epsilon) = \sum_{i=1}^{557} \frac{[\mu(\epsilon; z_i)_{theoretical} - \mu(z_i)_{observational}]^2}{\sigma(z_i)^2}, \quad (20)$$

where $\sigma(z_i)$ is the correspondent 1σ uncertainty. The observational data are consistent with the considered model if $\frac{\chi^2}{N-m} \leq 1$, where N is the range of the data set used, and m is the number of parameters.

In the table I we show that χ^2 values that we find for different values

ϵ	0.01	0.1	0.5	0.6	0.7
χ^2	546.97	545.70	543.82	544.23	544.97

Table I

for the ϵ -parameter. Note that for all values of ϵ -parameter considered we have $\frac{\chi^2}{556} \leq 1$, that indicates the consistence of the model with the Supernova data, but the test is not conclusive in respect to the more adequate interval for the ϵ -parameter. Although, the range $0.5 \leq \epsilon \leq 0.6$ furnishes a better agreement.

On the other hand, with the universe expansion, the coupling reactions becomes inefficient. Neutral atoms are formed and the ionization fraction freezes out. The photons become free and the lack of further interactions preserves the density irregularities, imprinted on the photons field. Consequently, the density perturbations in the coupled baryon-photon fluid in the pre-recombination epoch are responsible by the dominant acoustic anisotropy in CMB. Applying the classical angular diameter distance to CMB, we can learn about cosmological parameters by observing the anisotropy acoustic peak locations.

The sound horizon scale is the maximum distance that a sound wave could have traveled in approximately 300.000 yrs from the beginning of the matter era until the time of recombination. The angular diameter distance translate the Θ angle into a multipole l , or a length scale. Therefore, one expects acoustic normal modes that are linked to the harmonic series of anisotropies.

In order to obtain the multipole spacing for cosmological models we need of the angular diameter distance, the sound horizon scale and the redshift at decoupling, that is the epoch when the physical imprint of the acoustic anisotropies in the CMB temperature pattern occurs, and the photon become unaffected by further interactions with the matter. The angular scale of the peaks of the angular power spectrum of the cosmic microwave background anisotropies is given by $\Theta_a = \frac{\pi}{l_a}$, where the multipole associated to the angular scale Θ_a is given by [32]

$$l_a = \pi \frac{r(z_{dec})}{r_s(z_{dec})}. \quad (21)$$

The $r(z_{dec})$ is the comoving distance at decoupling, and $r_s(z_{dec})$ is the comoving size of the sound horizon at decoupling, that obeys [37]

$$r_s(z_{dec}) = \int_0^{\frac{1}{1+z_{dec}}} \frac{\overline{C}_s(R) dR}{R^2 H(R)}, \quad (22)$$

where the average sound speed before last scattering is given by $\overline{C}_s(a) = \frac{1}{\sqrt{3 + \frac{9\Omega_b}{4\Omega_\gamma} R}}$, and Ω_b , Ω_γ are the ratio for baryons and radiation, respectively.

The component of the dark energy can be taken negligible in the calculus of the sound horizon, and numerical simulations indicates an error of order of $10^{-5}\%$, resulting [37]

$$r_s = \frac{4}{3H_0} \frac{\Omega_\gamma}{\Omega_{dm0}\Omega_b} \ln \frac{[1 + A_{dec}]^{1/2} + [A_{dec} + A_{eq}]^{1/2}}{1 + A_{eq}^{1/2}}, \quad (23)$$

where $A = \frac{3\Omega_b}{4\Omega_\gamma} R$.

With help of Eqs. (17) and (20) we can show the profile for the multipole associated to the angular scale Θ_a , as function of the ϵ parameter (Fig.5). We consider the decoupling redshift $z_{dec} = 1089$ and the acoustic scale as 300 ± 3 [32]. So, we can infer an interval for the ϵ parameter, namely $\epsilon = 0.58 - 0.60$.

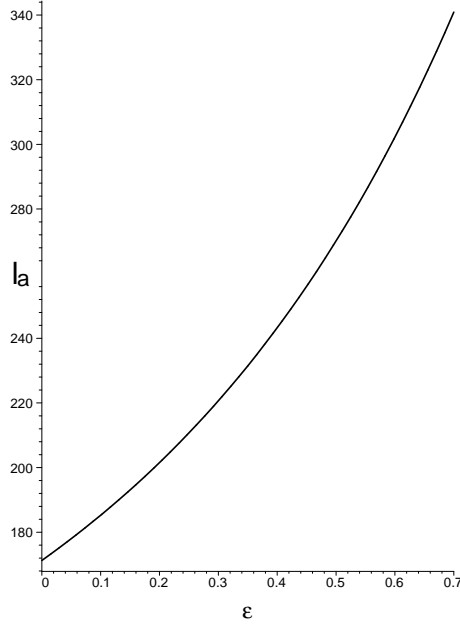


Figure 6: Acoustic scale as function of the ϵ -parameter.

The baryon acoustic oscillations(BAO) occurs at relatively large scales, but acoustic signature has been detected at low redshift using 2dF Galaxy Redshift Survey [33], and the Sloan Digital Sky Survey [34], estimating the distance-redshift relation at $z = 0.2$ and $z = 0.35$, respectively. The observed scale of the BAO calculated from these samples are analyzed and used to constrain the form of the distance

$$D_v(z) = [(1+z)^2 D_a^2(z) \frac{z}{H(z)}]^{1/3}, \quad (24)$$

where $D_A(z) = \frac{d_L(z)}{(1+z)^2}$ is the proper angular diameter distance, and $d_L(z)$ is the luminosity distance.

Matching the BAO to acquire the same measured scale at all redshifts we have [35], [36]

$$\chi_{BAO}^2 = \frac{[\frac{D_v(0.35)}{D_v(0.2)} - 1736]^2}{0.065^2}, \quad (25)$$

that allow us to find the reduced χ_{BAO}^2 for different ϵ values (Table II).

Note in the table II that the BAO at low redshifts indicates $\epsilon > 0.5$, in

ϵ	0.01	0.1	0.5	0.6	0.7
χ_{BAO}^2	1.27	1.14	0.9	0.79	0.79

Table II: Reduced χ_{BAO}^2 .

concordance with the BAO at large redshifts.

The validity interval that we find for the ϵ -parameter states how essential is the coupling between the dark components, and also indicates that the addition of a cosmological constant, possibly cannot describe the dynamics of the universe.

In several opportunities in the literature, the Λ -CDM model appear with good agreement to the observational data, and by several authors the model is considered as a paradigm. In the analyses of the different models, the statefinder parameters, introduced by Shani, Saini and Starobinsky [38], furnishes an qualitative idea, an geometrical diagnostic [39], [40] of how much the considered model is “distant” of the Λ -CDM. The statefinder pair is defined by:

$$r = \frac{d^3 R/dt^3}{(RH^3)}, \quad (26)$$

$$s = \frac{r-1}{3(q-\frac{1}{2})}. \quad (27)$$

For LCDM (Lambda cold dark matter model) model $\{r, s\} = \{1, 0\}$ is a fixed point and the departure from this point increase the distance from flat LCDM model [39].

It is not difficult express the statefinder parameter r in terms of the deceleration parameter and your redshift derivative, namely

$$r = 2q^2 + q + q'(1 + z). \quad (28)$$

Consequently, the expressions for the statefinder parameters $r(t)$ and $s(t)$ are, respectively:

$$r(t) = 1 + \frac{\epsilon^2 - 3\epsilon}{2\{\cosh \sqrt{KI}(\epsilon - 3)t/2\}^2 + (\epsilon - 3)} \quad (29)$$

$$s(t) = \frac{(3 - \epsilon)\epsilon}{3\{\cosh \sqrt{KI}(\epsilon - 3)t/2\}^2} \quad (30)$$

In the Fig.(7) we display the profile $s \times r$, and we note the sensibility of the statefinder parameters for relatively close values for the ϵ -parameter. Note that for high redshift the statefinder parameters of the interacting model that we study is close to point $\{1,0\}$, characteristic for the LCDM model.

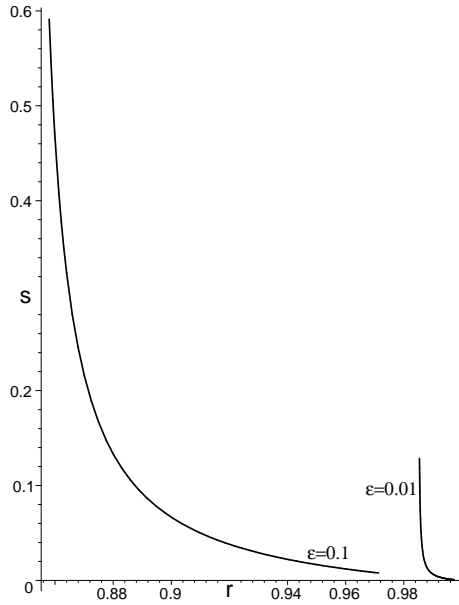


Figure 7: Time evolution of the statefinder pair $\{r,s\}$ for $\epsilon = 0.01$ and $\epsilon = 0.1$.The direction for the increasing redshift is identical to the direction of the increasing ϵ -parameter.

4 Conclusions

In this work we consider a coupling between the dark components of the universe, where the dark matter density will dilute in a different rate. So, we have creation of dark matter particles at expenses of dark energy, and the ϵ -parameter is linked to the creation process. An interesting feature of the models with only one parameter is related to the coincidence problem, that contrary to a cosmological principle stating that we are in a special era of the universe. With only one parameter governing the dynamics the coincidence problem is alleviated, and in some sense eliminated. Taking into account the Union Sample of 557 Supernova Ia, 2dF Galaxy Redshift Survey and the Sloan Digital Sky Survey, we find $0.5 \leq \epsilon \leq 0.6$, considering the first experiment, and $\epsilon \geq 0.5$ for the second and third experiments. The interval obtained in the cited experiments do not contradict the provisions for the age of the universe, but the transition redshift obtained have a highest value than the established in the present literature.

Acknowledgements

The author acknowledges the suggestions of the anonymous referee to the paper.

References

- [1] M. L. Krauss and M. Turner, *Gen. Relativ. Gravit.*, **27**, 1137, (1996).
- [2] A. G. Riess et al., *Astron. J.*, **116**, 1009, (1998).
- [3] S. Perlmutter et al., *Astrophys. J.*, **517**, 565, (1999).
- [4] D. N. Spergel et al., *Astrophys. J. Suppl. Ser.*, **170**, 377, (2007).
- [5] A. G. Riess et al., *Astrophys. J.*, **607**, 665, (2004).
- [6] S. Weinberg, *Rev. Mod. Phys.*, **61**, 1009, (1989).
- [7] J. Garrig and A. Vilenkin, *hep-th/00011262*, (2000).
- [8] G. Efstathiou, *Mon. Not. R. Astron. Soc.*, **274**, L73, (1995).
- [9] Carrol S. M., *Living Rev. Rel.*, **4**, 1, (2001).
- [10] Peebles P. J. and B. Ratra, *Rev. Mod. Phys.*, **75**, 559, (2003).
- [11] Harvard B. Sandvik, Max Tegmark, Matias Zaldarriaga and Ioav Zaga, *Phy. Rev. D*, **69**, 123524, (2004).

- [12] T. Padmanabhan and T. Roy. Choudhury, *Phy. Rev. D*, **66**, 081301, (2003).
- [13] I. Prigogine, J. Gehehiau, E. Gunzig and P. Nardone, *Gen. Relativ. Gravit.*, **21**, 767 (1989).
- [14] J. A. S. Lima, A. S. M. Germano and L. R. W. Abramo, *Phy. Rev D*, **53**, 4287, (1996).
- [15] J. A. S. Lima, *Phy. Rev. D*, **54**, 2571, (1996).
- [16] W. McCrea, *Proc. R. Soc. London A*, **206**, 562 (1951).
- [17] Pereira S. H. and Jesus J. E., *Phy. Rev. D*, **79**, 043517 (2009).
- [18] C. Feng, B. Wang, E. Abdalla and R. K. Su, *Phys. Lett. B*, **665**, 111 (2008).
- [19] D. Pavon and B. Wang, *Gen. Relativ., Gravit.*, **41**, 1 (2009).
- [20] P. Wang and X. Meng, *Class. Quant. Grav.*, **22**, 283 (2005).
- [21] J. A. Lima, *Braz. J. Phys.*, **34**, 194 (2004).
- [22] D. N. Spergel, *Astrophys. J. Suppl. Ser.*, **148**, 175, (2003).
- [23] J. C. Carvalho, J. A. Lima and I. Waga, *Phy. Rev. D*, **46**, 2404, (1992).
- [24] J. S. Alcaniz and J. A. S. Lima, *Phy. Rev. D*, **72**, 063516, (2006).
- [25] L. Knox, N. Christensen and C. Skordis, *Astrophys. J.*, **563**, L95 (2003).
- [26] W. Hu, M. Fukugita, , M. Zaldarriaga and M. Tegmark, *Astrophys. J.*, **549**, 669 (2001).
- [27] Bin Wang, Jiadong Zang, Chi-Yong Lin, Elcio Abdalla and S. Micheletti, *Nuclear Physics B*, **778**, 69 (2007).
- [28] J. M. Virey, *Phys. Rev. D*, **72**, 061312(R) (2005).
- [29] A. Friaca, J. S. Alcaniz and J. A. S. Lima, *Mon. Not. R. Astron. Soc.*, **362**, 1295 (2005).
- [30] L. M. Krauss and B. Chaboyer, *Science*, **299**, 65 (2003).
- [31] Amanullah et al., arXiv:1004.1711.
- [32] L. Page et al., *Astrophys. J. Suppl. Ser.*, **148**, 233 (2003).
- [33] M. Coles, *astro-ph/0306581*, (2003).

- [34] D. G. York, *Astrophys. J.*, **120**, 1579 (2010); arXiv:1004.1711.
- [35] Amanullah et al., arXiv:0907.1660.
- [36] J. Lu, E. N. Saridakis, M.R. Setare and L. Xu, *JCAP*, **1003**, 031, (2010).
- [37] Wayne Hu and Naoshi Sugiyama, *Astrophys. J.*, **444**, 489 (1995).
- [38] V. Shani, T. D. Saini, A. A. Starobinsky and U. Alam, *JETP Lett.*, **77**, 201 (2003).
- [39] U. Alam, Varun Sahni, Tarun Deep Saini and A. A. Starobinsky, *Mon. Not. R. Astron. Soc.*, **344**, 1057 (2003).
- [40] Jingfei Zhang, Xin Zhang and Hongya Lin, *Phys. Lett.*, **B659**, 26-33 (2008).
- [41] J. B. Binder and G. M. Kremer, *Gen. Rel. Grav.* **38**, 857 (2006); [*gr-qc/0601105*].
- [42] D. Tocchini-Valentini and L. Amendola, *Phys. Rev. D* **65**, 063508 (2002); [*astro-ph/0108143*].
- [43] G. R. Farrar and P. J. E. Peebles, *Astrophys. J.* **604**, 1 (2004); [*astro-ph/0307316*].
- [44] G. M. Kremer, *Gen. Rel. Grav.* **39**, 965-972 (2007); [*gr-qc/0704.0371*].
- [45] G. Huey and B. D. Wandelt, *Phys. Rev. D* **74**, 023519 (2006); [*astro-ph/0407196*].
- [46] G. Mangano, G. Miele and V. Pettorino, *Mod. Phys. Lett. A* **18**, 831 (2003); [*astro-ph/0212518*].
- [47] L. P. Chimento and M. Forte, [*astro-ph/07064142*].
- [48] R. G. Cai and A. Wang, *JCAP* **0503**, 002 (2005). [*hep-th/0411025*].
- [49] L. Amendola, *Phys. Rev. D* **62**, 043511 (2000); [*astro-ph/9908023*].
- [50] L. Amendola and D. Tocchini-Valentini, *Phys. Rev. D* **64**, 043509 (2001); [*astro-ph/0011243*].
- [51] L. Amendola and D. Tocchini-Valentini, *Phys. Rev. D* **66**, 043528 (2002); [*astro-ph/0111535*].
- [52] L. Amendola, C. Quercellini, D. Tocchini-Valentini and A. Pasqui, *Astrophys. J.* **583**, L53 (2003). [*astro-ph/0205097*].
- [53] S. Nesseris and L. Perivolaropoulos, *Phys. Rev. D*, **77**, 023504, (2008).
- [54] J. A. Lima, *Phys. Rev. D*, **54**, 2571, (1996).